

Bethe-Salpeter amplitudes of Upsilon

Rasmus Larsen,¹ Stefan Meinel,^{2,3} Swagato Mukherjee,¹ and Peter Petreczky¹

¹*Physics Department, Brookhaven National Laboratory, Upton, New York 11973, USA.**

²*Department of Physics, University of Arizona, Tucson, Arizona, USA.*

³*RIKEN-BNL Research Center, Brookhaven National Laboratory, Upton, New York 11973, USA.*

(Dated: December 17, 2020)

Based on lattice non-relativistic QCD (NRQCD) studies, we present results for Bethe-Salpeter amplitudes for $\Upsilon(1S)$, $\Upsilon(2S)$, and $\Upsilon(3S)$ in vacuum as well as in quark-gluon plasma. Our study is based on $2+1$ flavor $48^3 \times 12$ lattices generated using the Highly Improved Staggered Quark (HISQ) action and with a pion mass of 161 MeV. At zero temperature the Bethe-Salpeter amplitudes follow the expectations based on non-relativistic potential models. At non-zero temperatures, the interpretation of Bethe-Salpeter amplitudes turns out to be more nuanced but consistent with our previous lattice QCD study of excited Upsilon in quark-gluon plasma.

I. INTRODUCTION

Potential models give a good description of the quarkonium spectrum below the open charm and bottom thresholds; see e.g., Refs. [1, 2] for reviews. Even some of the states above the threshold are also reproduced well within this model. Potential models can be justified using an effective field theory approach [3, 4]. This approach is based on the idea that for a heavy quark with mass m , there is a separation of energy scales related to the quark mass, inverse size of the bound state, and binding energy, $m \gg mv \gg mv^2$, with v being the velocity of the heavy quark inside the quarkonium bound state. The effective field theory at scale mv is the non-relativistic QCD (NRQCD), where the heavy quark and anti-quark are described by non-relativistic Pauli spinors and pair creation is not allowed in this theory [5]. The effective theory at scale mv^2 is potential NRQCD (pNRQCD), and the quark anti-quark potential appears as a parameter of the pNRQCD Lagrangian. Potential model appears as the tree level approximation of pNRQCD [4]. Non-potential effects are manifest in the higher order corrections. For very large quark mass, $v \sim \alpha_s \ll 1$. Therefore, the large energy scales can be integrated out perturbatively [3, 4]. However, for most of the quarkonium states realized in nature this condition is not fulfilled. If $\Lambda_{QCD} \gg mv^2$, all the energy scales can be integrated out non-perturbatively and the potential is given in terms of Wilson loops calculated on the lattice [3, 4]. So, in this limit, too, the potential description is justified. However, for many quarkonia, $\Lambda_{QCD} \simeq mv^2$, and it is not clear how to justify the potential models.

In potential models, one can also calculate the quarkonium wave function. On the other hand, in lattice QCD we can calculate the Bethe-Salpeter amplitude, which in the non-relativistic limit reduces to the wave function. Thus, one can use the Bethe-Salpeter amplitude for further tests of the potential models. In particular, one can also reconstruct the potential from the Bethe-Salpeter

amplitude [6–10]. Most of these studies focused on quark masses close to or below the charm quark mass, though in Ref. [9] quark masses around the bottom quark have also been considered. The resulting potential turned out to be similar to the static potential calculated on the lattice, but some differences have been found. The potential description is expected to work better for larger quark masses, and therefore the bottomonium is best suited for testing this approach. Studying the bottomonium on the lattice using a fully relativistic action is more difficult because of the large cutoff effects and the rapid fall-off of the correlators. One of our aims is to test the potential model by calculating the bottomonium Bethe-Salpeter amplitude using lattice NRQCD [11, 12], which is very well suited for studying the bottomonium [13–20].

The existence and the properties of quarkonia in the hot medium attracted a lot of attention in the last 30 years. It was proposed a long time ago that quarkonium production in heavy-ion collisions can be used to probe quark-gluon plasma (QGP) formation [21]. The study of in-medium properties of quarkonia and their production in heavy ion collisions is an extensive research program; see e.g., Refs. [22–24] for reviews. The in-medium properties of quarkonia as well as their dissolution (melting) are encoded in the finite temperature spectral functions. Quarkonium states show up as peaks in the spectral function that become broader as the temperature increases and eventually disappear above some temperature (T). The temperature above which no peaks in the spectral function can be identified is often called the melting temperature. Reconstructing quarkonium spectral functions from lattice calculations at non-zero temperature appeared to be very challenging (see, e.g., discussions in Refs. [25–28]). The study of Bethe-Salpeter amplitudes has been proposed as an alternative method to address this problem. The idea behind this approach is to compare the Bethe-Salpeter amplitude calculated on the lattice with the expectations of the free field theory that would indicate an unbound heavy quark anti-quark pair. Bethe-Salpeter amplitudes at non-zero temperature for charmonium have been calculated in previous lattice QCD studies [29–34], but presently our understanding re-

* rlarsen@bnl.gov

garding the interpretations of quarkonia Bethe-Salpeter amplitudes at $T > 0$ remains murky. Although using a weak-coupling approach it is possible to generalize the potential description to non-zero temperature [35, 36], it is unclear if such an approach and the interpretations of quarkonia Bethe-Salpeter amplitudes are applicable in the temperature regime of interest. In this paper, we focus on lattice NRQCD based determinations of Bethe-Salpeter amplitudes of $\Upsilon(1S)$, $\Upsilon(2S)$, and $\Upsilon(3S)$ states at $T > 0$. By comparing with the corresponding $T = 0$ results, where the interpretations of Bethe-Salpeter amplitudes are more straightforward, we point out and discuss subtleties associated with interpretations of Bethe-Salpeter amplitudes at $T > 0$.

II. BETHE-SALPETER AMPLITUDES AT $T = 0$

To define the Bethe-Salpeter amplitude for the bottomonium we consider the correlation function

$$\tilde{C}_\alpha^r(\tau) = \left\langle O_{qq}^r(\tau) \tilde{O}_\alpha(0) \right\rangle, \quad (1)$$

where \tilde{O}_α is the meson operator that has a good overlap with a given quarkonium state α and O_{qq}^r is a point-split meson operator with the quark and antiquark fields separated by distance r ,

$$O_{qq}^r(\tau) = \sum_{\mathbf{x}} \bar{q}(\mathbf{x}, \tau) \Gamma q(\mathbf{x} + \mathbf{r}, \tau). \quad (2)$$

Here, Γ fixes the quantum number of the meson. Furthermore, in the present work we use Coulomb gauge fixed ensembles to define the expectation value. Inserting a complete set of states we obtain the following spectral decomposition of the correlator:

$$\tilde{C}_\alpha^r(\tau) = \sum_n \langle 0 | O_{qq}^r(0) | n \rangle \langle n | \tilde{O}_\alpha(0) | 0 \rangle e^{-E_n \tau}. \quad (3)$$

Assuming that only one state $|\alpha\rangle$ contributes at large τ , which is correct for an appropriately chosen \tilde{O}_α , at large Euclidean time we have

$$\tilde{C}_\alpha^r(\tau) = A_\alpha^* \langle 0 | O_{qq}^r(0) | \alpha \rangle e^{-E_\alpha \tau}, \quad (4)$$

where $A_\alpha^* = \langle \alpha | \tilde{O}_\alpha(0) | 0 \rangle$. The matrix element

$$\phi_\alpha(r) = \langle 0 | O_{qq}^r(0) | \alpha \rangle \quad (5)$$

is called the Bethe-Salpeter (BS) amplitude and describes the overlap of the quarkonium state $|\alpha\rangle$ with the state that is obtained by letting the two field operators at distance r act on the vacuum. In the non-relativistic limit, it reduces to the wave function of the given quarkonium state. Thus, up to normalization factor, the Bethe-Salpeter amplitude is given by the large τ behavior of $\exp(E_\alpha \tau) C_\alpha^r(\tau)$, with E_α being the energy of quarkonium state $|\alpha\rangle$, which is also calculated on the lattice. In the

following, we will use the terms BS amplitude and wave function interchangeably.

As mentioned in the Introduction, we aim to calculate the bottomonium BS amplitudes using NRQCD. We performed calculations using 2+1 flavor gauge configurations generated by HotQCD with the highly improved staggered quark (HISQ) action [37, 38]. The strange quark mass was fixed to its physical value, while the light quark masses correspond to the pion mass of 161 MeV in the continuum limit [37, 38]. We use the same NRQCD formulation as in our previous study [39, 40]. For the calculations at zero temperature, we use 48^4 lattices and $\beta = 10/g_0^2 = 6.74$ corresponding to lattice spacing $a = 0.1088$ fm. We use 192 gauge configurations in our analysis with eight sources per configuration.

To construct the meson operators that have the optimal projection we start with the source [40]

$$O_i(\tau, \mathbf{x}) = \sum_{\mathbf{r}} \psi_i(\mathbf{r}) \bar{q}(\tau, \mathbf{x}) \Gamma q(\tau, \mathbf{x} + \mathbf{r}). \quad (6)$$

Here, $\psi_i(r)$ is the trial wave function of the i th bottomonium state obtained by solving the Schrödinger equation with the Cornell potential modified by discretization effects [15]. Since $G_{ij}(\tau) = \langle O_i(\tau) O_j(0) \rangle$ is non-zero (though small) also for $i \neq j$, we have to solve the generalized eigenvalue problem

$$G_{ij}(\tau) \Omega_{j\alpha} = \lambda_\alpha(\tau, \tau_0) G_{ij}(\tau_0) \Omega_{j\alpha} \quad (7)$$

to obtain the optimized operator for bottomonium state α ,

$$\tilde{O}_\alpha = \sum_j \Omega_{j\alpha} O_j. \quad (8)$$

The value of τ_0 is arbitrary to some extent but should be considerably smaller than τ . Choosing larger τ_0 helps suppressing higher lying states, i.e., states with energies larger than the energy of $\Upsilon(3S)$. However, the operators O_i in Eq. (6) already have very good overlap with $\Upsilon(nS)$ states. Therefore, we choose $\tau_0 = 0$ in this study. It has been checked in our previous work that using larger values of τ_0 does not change the results significantly [40]. To obtain the BS amplitude, we consider the large τ behavior of the following combination:

$$e^{E_\alpha \tau} \tilde{C}_\alpha^r(\tau) = e^{E_\alpha \tau} \sum_j \Omega_{j\alpha} \langle O_{qq}^r(\tau) O_j(0) \rangle. \quad (9)$$

The energy E_α has been determined from the fits of the correlators of the optimized operators \tilde{O}_α [40]. In practice, the value of τ does not have to be very large. We find that $\tau > 0.3$ fm works for all states; i.e., the resulting BS amplitudes are time independent. For $\tau = 0$ the BS amplitude will be equal to the trial wave function $\psi_i(r)$. To obtain the proper normalization of the BS amplitude we require that $\int_0^\infty dr r^2 |\phi_\alpha(r)|^2 = 1$. After this normalization exponential factor $e^{E_\alpha \tau}$ drops out. Therefore, the normalized BS amplitudes do not depend on the

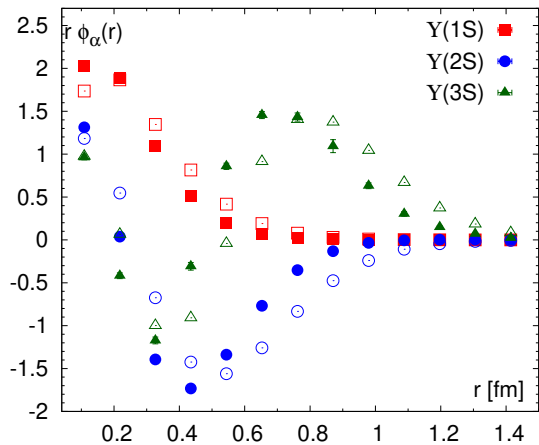


FIG. 1. The BS amplitudes for $\Upsilon(1S)$, $\Upsilon(2S)$, and $\Upsilon(3S)$ states at $T = 0$ as function of r (filled symbols) compared with the corresponding trial wave functions (open symbols).

choice of the energy E_α . In Fig. 1 we show the BS amplitude $\phi_\alpha(r)$ for $\Upsilon(1S)$, $\Upsilon(2S)$ and $\Upsilon(3S)$ states compared to the corresponding trial wave functions $\psi_\alpha(r)$ used to construct the optimized meson operators. We see that the r -dependence of the BS amplitudes is in qualitative agreement with the expectations of non-relativistic potential model. However, the details of the r dependence are different from the input trial wave function. We also note that the orthogonalization procedure is important for getting the correct r dependence of the BS amplitudes.

If the potential picture is valid the BS amplitude should satisfy the Schrödinger equation

$$\left(\frac{-\nabla^2}{m_b} + V(r)\right)\phi_\alpha = E_\alpha\phi_\alpha, \quad (10)$$

with m_b being the b -quark mass of the potential model. Note that the reduced mass in the $b\bar{b}$ system is $m_b/2$, hence the absence of factor two in the above equation. Using the BS amplitude and the energy of at least two bottomonia states determined in NRQCD from the above equation we can obtain m_b and the potential $V(r)$. We determine the b -quark mass using $\Upsilon(1S)$ and $\Upsilon(2S)$ states as follows

$$m_b = \frac{\frac{\nabla^2\phi_{\Upsilon(1S)}}{\phi_{\Upsilon(1S)}} - \frac{\nabla^2\phi_{\Upsilon(2S)}}{\phi_{\Upsilon(2S)}}}{E_{\Upsilon(2S)} - E_{\Upsilon(1S)}} \quad (11)$$

To evaluate $\nabla\phi_\alpha$ we use the simplest difference scheme. The value of m_b determined from the above equation for different values of quark antiquark separation r is shown in Fig. 2. The r -range was chosen such that it does not include the node of $\Upsilon(2S)$ and large distances, where the statistical errors are large. We see some modulation of the extracted m_b in r , which may indicate that the BS amplitude cannot be completely captured by the

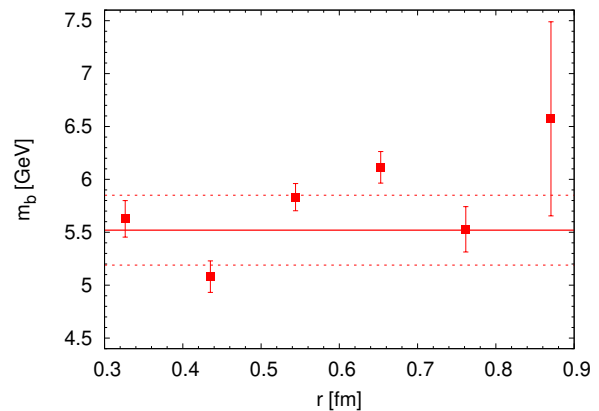


FIG. 2. The effective bottom quark mass, m_b , in the potential approach determined for different quark antiquark separations r (see text). The horizontal solid line is the fitted value of m_b , while the dashed lines indicate the corresponding uncertainty.

Schrödinger equation, but there is no clear tendency of m_b as function of r . Therefore we fitted the values of m_b obtained for different r to a constant. This resulted in

$$m_b = 5.52 \pm 0.33 \text{ GeV}. \quad (12)$$

This value of the effective bottom quark mass obtained by us is not very different from the one used by the original Cornell model, $m_b = 5.17$ GeV [41], but is significantly larger than the b -quark mass used in most of the potential models (see, e.g., Ref. [42]). We also determined the value of m_b using the BS amplitudes and the energy levels of $\Upsilon(1S)$ and $\Upsilon(3S)$ and obtained $m_b = 5.82(0.51)$ GeV. This agrees with the above result within the errors.

Having determined m_b , we can also calculate the potential, $V(r)$, using the BS amplitudes and the bottomonium energy levels as

$$V(r) = E_\alpha + \frac{\nabla^2\phi_\alpha}{m_b\phi_\alpha}. \quad (13)$$

The results are shown in Fig. 3. Given our findings for m_b , it is not surprising that the values of the potential obtained using $\Upsilon(1S)$, $\Upsilon(2S)$, and $\Upsilon(3S)$ states agree within errors. In the figure, we also compare the value of $V(r)$ determined from the different states to the phenomenological potential of the original Cornell model [41] and the energy of static quark antiquark pair obtained from Wilson loops at lattice spacing $a = 0.06$ fm [38]. It is quite non-trivial that all these potentials agree with each other. A similar conclusion is reached in Refs. [7–9] when the limit of quark mass going to infinity is taken. We note that the relativistic corrections to the spin-dependent part of the potential are quite small for the b quark mass [43] and thus are not visible given our statistical errors.

The discussion above ignored spin-dependent effects. To address the spin-dependent part of the potential we also calculated the BS amplitude for $\eta_b(nS)$ states, $n =$

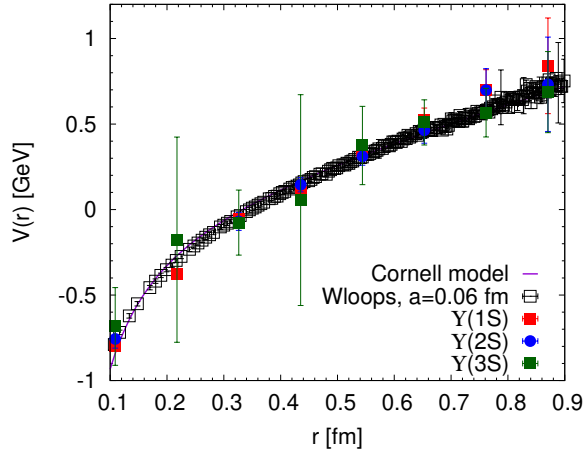


FIG. 3. The potential, $V(r)$, obtained from the BS amplitude of $\Upsilon(1S)$, $\Upsilon(2S)$ and $\Upsilon(3S)$ states compared to the phenomenological Cornell potential [41] shown as a solid line as well as to the energy of the static quark antiquark pair obtained from Wilson loops using $a = 0.06$ fm lattice [38]. All the lattice results were normalized to coincide with the Cornell potential at $r = 0.4$ fm.

1, 2, 3. We have found that the corresponding BS amplitudes agree with the ones of the $\Upsilon(nS)$ states within errors. Therefore, with the present statistics, we cannot resolve the spin-dependent part of the potential.

As discussed above, the r -dependence of the BS amplitudes qualitatively follow the r -dependence of the trial wave function $\psi_i(r)$ obtained from the potential model. But at qualitative level, significant differences can be seen, (cf. Fig. 1). This potential model used $m_b = 4.676$ GeV [15], which is smaller than the effective quark masses determined above. Therefore, we calculated the wave functions of (nS) bottomonium states using the static quark anti-quark energy [38] as a potential and $m_b = 6$ GeV. The results are shown in Fig. 4 and we see that the agreement between the BS amplitude and the wave functions is significantly improved. We also note that the dependence of the energy levels on m_b is rather mild; e.g., changing m_b from 4 to 6 GeV only reduces the spin-averaged 2S-1S splitting by 3.5%. Thus, using large values of m_b in the potential model is a viable option.

III. BETHE-SALPETER AMPLITUDES AT $T > 0$

We can also consider the mixed correlator $\tilde{C}_\alpha^r(\tau, T)$ defined in Eq. (1) for $T > 0$ by evaluating the expectation value over a thermal ensemble at a temperature $T = 1/\beta$,

$$\tilde{C}_\alpha^r(\tau, T) = \frac{1}{Z(\beta)} \text{Tr} \left[O_{qq}^r(\tau) \tilde{O}_\alpha(0) e^{-\beta H} \right], \quad (14)$$

with the thermal partition function $Z(\beta) = \text{Tr} [e^{-\beta H}]$. Using energy eigenstates to evaluate the trace and inserting a complete set of states we obtain the following

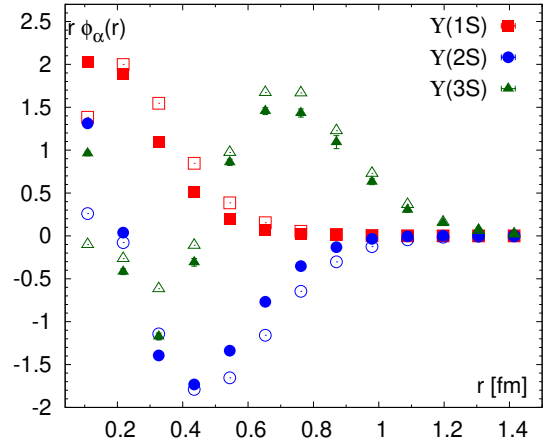


FIG. 4. The BS amplitude for $\Upsilon(nS)$ states as function of r (filled symbols) compared with the non-relativistic wave functions obtained from potential model with $m_b = 6$ GeV (open symbols).

expression for the correlator $\tilde{C}_\alpha^r(\tau, T)$:

$$\tilde{C}_\alpha^r(\tau, T) = \frac{1}{Z(\beta)} \sum_{n,m} e^{-(E_n - E_m)\tau} \langle m | O_{qq}^r | n \rangle \langle n | \tilde{O}_\alpha | m \rangle e^{-\beta E_m}. \quad (15)$$

Since we perform calculations in NRQCD, the sum over m should be restricted to states that do not contain the heavy quark anti-quark pair; heavy quark pair creation is not allowed in NRQCD. We denote those states as $|m'\rangle$. If we write the states $|n\rangle$ as $|n'\gamma\rangle$, where index n' labels the light degrees of freedom and γ labels the quarkonium states, the above expression for $\tilde{C}_\alpha^r(\tau, T)$ can be rewritten as

$$\tilde{C}_\alpha^r(\tau, T) = \frac{1}{Z(\beta)} \sum_{\gamma, n', m'} \left[e^{-(E_{n',\gamma} - E_{m'})\tau} e^{-\beta E_{m'}} \langle m' | O_{qq}^r | n'\gamma \rangle \langle n'\gamma | \tilde{O}_\alpha | m' \rangle \right]. \quad (16)$$

If we write $E_{m'\gamma} = E_\gamma + E_{m'} + \Delta E_{m'\gamma}$ and assume that the operator \tilde{O}_α mostly projects onto quarkonium state $|\alpha\rangle$, we can obtain a simplified form,

$$\tilde{C}_\alpha^r(\tau, T) = e^{-E_\alpha \tau} \left[\phi_\alpha A_\alpha^{*'} + \frac{1}{Z(\beta)} \sum_{m'} \langle m' | O_{qq}^r | m' \alpha \rangle \langle m' \alpha | \tilde{O}_\alpha | m' \rangle e^{-\beta E_{m'} - \Delta E_{m'\alpha} \tau} \right] \quad (17)$$

with $A_\alpha^{*'} = A_\alpha^*/Z(\beta)$. In the above equation, we separated out the $m' = 0$ vacuum contribution in the sum corresponding to the thermal trace. At small temperature, the first term in the above equation is the dominant one, and the correlator is approximately given by the $T = 0$ BS amplitude. In general, however, there is no simple interpretation of the correlator $\tilde{C}_\alpha^r(\tau, T)$ in terms of

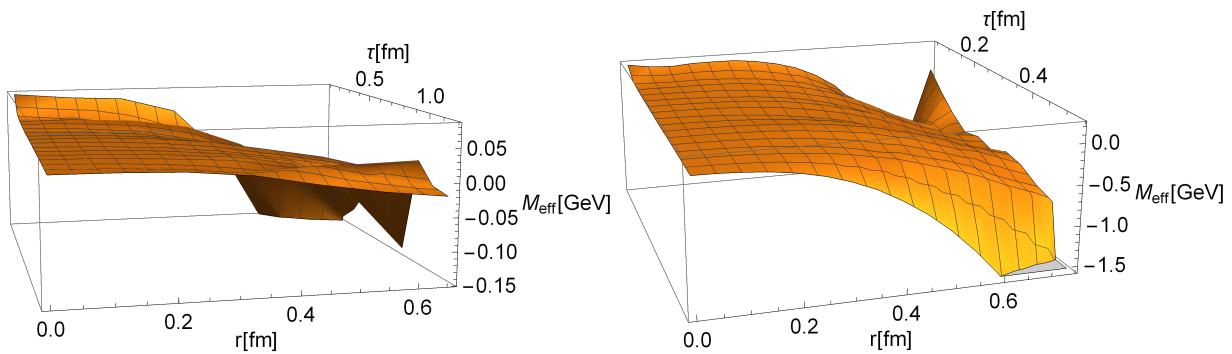


FIG. 5. The effective masses $M_{\text{eff}}^r(\tau, T)$ in GeV of the $\Upsilon(1S)$ correlator at $T = 151$ MeV (left) and $T = 334$ MeV (right) as function of τ and r .

β	T (MeV)	Number of configs.
6.740	151	384
6.880	172	384
7.030	199	384
7.280	251	384
7.596	334	384

TABLE I. The parameters for the 2+1 flavor HISQ ensembles at $T > 0$ with $48^3 \times 12$ lattices.

some finite temperature quarkonium wave function. The temperature dependence of this correlator crucially depends on the value of the matrix elements $\langle m' | O_{qq}^r | m' \alpha \rangle$ and $\langle m' \alpha | \tilde{O}_\alpha | m' \rangle$. The size of $\langle m' | O_{qq}^r | m' \alpha \rangle$ depends on the separation r and therefore, also the size of the thermal effect will be r dependent. For values of r that are about the size of the bottomonium state of interest the matrix elements $\langle m' | O_{qq}^r | m' \alpha \rangle$ and $\langle m' \alpha | \tilde{O}_\alpha | m' \rangle$ should be of similar size, and thus the temperature dependence of $\tilde{C}_\alpha^r(\tau, T)$ is expected to be comparable to the correlator of \tilde{O}_α explored in Ref. [40].

We performed calculations of \tilde{C}_α^r at six different temperatures using $48^3 \times 12$ lattices from HotQCD collaboration. The parameters of the calculations including the gauge coupling $\beta = 10/g_0^2$ and number of configurations are summarized in Table I. As at zero temperature, we used 8 sources per gauge configuration. The projection matrix $\Omega_{j\alpha}$ has been determined from the finite temperature correlators according to Eq. (7). We checked, however, that the difference between the finite temperature projection matrix and the zero temperature projection matrix is very small.

We could use the same approach as in Ref. [40] to explore the temperature dependence of the correlator $\tilde{C}_\alpha^r(\tau, T)$ and define the effective mass for a fixed r ,

$$aM_{\text{eff}}^r(\tau, T) = \ln \left(\frac{\tilde{C}_\alpha^r(\tau, T)}{\tilde{C}_\alpha^r(\tau + a, T)} \right). \quad (18)$$

Now, the effective mass also depends on the distance r between the quark and antiquark in the point-split cur-

rent. In Fig. 5, we show the effective mass of $\Upsilon(1S)$ correlator as function of r and τ at the lowest and the highest temperature. The errors of the effective masses are not shown to improve the visibility. Since the energy levels in NRQCD are only defined up to a lattice spacing dependent constant, as in Ref. [39], we calibrate the effective masses with respect to the energy level of $\eta_b(1S)$ state at zero temperature. At large τ and r , the errors are quite large, and within these errors we do not see any medium effects in the effective mass at the lowest temperature. For small r , the effective mass quickly reaches a plateau with increasing τ . For large r , the effective mass at 151 MeV reaches the plateau from below. At the highest temperature, $T = 334$ MeV, the r and τ dependences of the effective masses looks similar for not too large values of r . However, the behavior of the effective mass is qualitatively different for large r . In particular, the effective mass does not reach a plateau with increasing τ . For excited states, the results for $M_{\text{eff}}^r(\tau, T)$ look similar, except that the errors are very large for $r > 0.65$ fm. As an example, we show the effective mass for $\Upsilon(3S)$ in Fig. 6 at two values of r , $r = 0.25$ fm and $r = 0.65$ fm for different temperatures. For the smaller r , we see no temperature dependence of the $\Upsilon(3S)$ effective mass at $T = 172$ MeV and $T = 251$ MeV. This is likely due to the fact that the matrix elements $\langle m' | O_{qq}^r | m' \Upsilon(3S) \rangle$ are small for $r = 0.25$ fm and the first term in Eq. (17) dominates. Note, however, that the errors are large. For the highest temperature, $T = 334$ MeV we start to see significant temperature dependence. For the larger distance, $r = 0.65$ fm, the medium effects are more pronounced. While the modifications of M_{eff}^r are small for $T = 172$ MeV, thermal effects are significant for $T = 251$ MeV and 334 MeV, comparable in size to the thermal effects in the effective masses of correlators of optimized operators [40].

Since the correlator \tilde{C}_α^r does not correspond to a positive definite spectral function, it is difficult to infer in-medium properties of bottomonia from M_{eff}^r . The large statistical errors make this even more complicated. Another way to analyze the temperature dependence of \tilde{C}_α^r

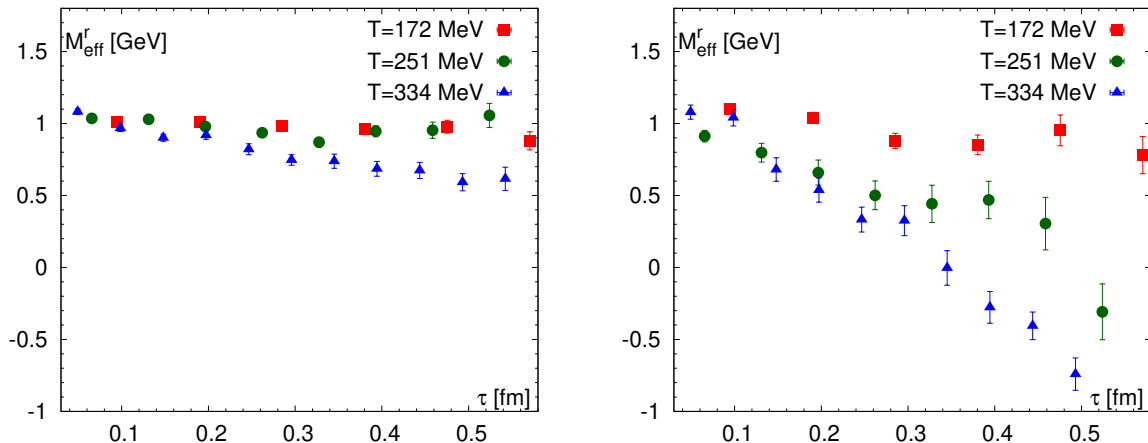


FIG. 6. The effective masses $M_{\text{eff}}^r(\tau, T)$ in GeV of the $\Upsilon(3S)$ correlator for $r \simeq 0.25$ fm (left) and $r \simeq 0.65$ fm (right) at different temperatures as function of τ .

is to consider the integral

$$N_{\alpha}(\tau, T) = \int_0^{\infty} dr r^2 \left(\tilde{C}_{\alpha}^r \right)^2. \quad (19)$$

At zero temperature, this quantity should be proportional to $\exp(-2E_{\alpha}\tau)$ for sufficiently large τ . This is also expected to be true below the crossover temperature. The combination

$$N_{\text{norm}}(\tau, T) = \exp(2E_{\alpha}\tau) N_{\alpha}(\tau, T) \quad (20)$$

should be independent of τ and can be interpreted as the normalization of the BS amplitude. In Fig. 7, we show $N_{\text{norm}}(\tau, T)$ as function of τ for different temperatures normalized to one at $t = \tau/a = 3$. As before, the energy values, E_{α} , have been determined from the correlators of optimized operators at $T = 0$ [40].

For the lowest temperature as well as for $T = 0$, we see that $N_{\text{norm}}(\tau, T)$ is approximately constant as expected. Here, we note that the τ range in Fig. 7 is different for $\Upsilon(1S)$, $\Upsilon(2S)$, and $\Upsilon(3S)$ states. This is due to the fact that the correlators $C_{\Upsilon(2S)}^r$ and $C_{\Upsilon(3S)}^r$ will be contaminated by the lowest $\Upsilon(1S)$ state at large τ as the projection is not perfect due to the small operator basis of only three operators used in this study. As the temperature increases we see that $N_{\text{norm}}(\tau, T)$ no longer approaches a constant but increases at large τ . This implies that the correlator \tilde{C}_{α}^r is no longer dominated by the first term in Eq. (17). The τ -dependence of $N_{\text{norm}}(\tau, T)$ is larger for high temperatures and is also more pronounced for excited states, as expected.

We could also analyze the τ -dependence of $N_{\alpha}(\tau, T)$ in terms of the corresponding effective masses

$$aM_{\text{eff}}^{N_{\alpha}}(\tau, T) = \ln \left(\frac{N_{\alpha}(\tau, T)}{N_{\alpha}(\tau + a, T)} \right). \quad (21)$$

At large τ these effective masses should reach a plateau equal to $2E_{\alpha}$. Our results for $M_{\text{eff}}^{N_{\alpha}}$ for the different

$\Upsilon(nS)$ states are shown in Fig. 8. As before the effective masses have been calibrated with respect to the energy of η_b state at $T = 0$. We see that at $T = 0$ as well as at the lowest temperature the effective masses reach a plateau corresponding to the physical mass (energy), but at higher temperatures this is not the case, in general. For the ground state the errors are large enough so that no clear medium shift can be seen, except at the highest temperature, $T = 334$ MeV. For the $\Upsilon(2S)$ the corresponding effective masses decrease with increasing τ for $T \geq 251$ MeV. For the $\Upsilon(3S)$ we see a significant shift in $M_{\text{eff}}^{N_{\alpha}}(\tau, T)$ already for $T > 191$ MeV. The behavior of $M_{\text{eff}}^{N_{\alpha}}(\tau, T)$ is qualitatively similar to the behavior of the effective masses of the correlator of optimized operators studied in Ref. [40]. This corroborates the findings of Ref. [40] on the in-medium modifications of the bottomonium spectral functions. For the $\Upsilon(1S)$ state our findings are also consistent with other studies of bottomonium at non-zero temperature using NRQCD [44–49].

Before concluding this section, we mention that so far we only discussed $\Upsilon(nS)$ states but very similar results have been obtained for $\eta_b(nS)$ states as well.

IV. COMPARISONS BETWEEN $T > 0$ AND $T = 0$ BETHE-SALPETER AMPLITUDES

If we insist on the interpretation of the correlator $\tilde{C}_{\alpha}^r(\tau, T)$ in terms of the wave function, we could simply divide it by $N_{\alpha}(\tau, T)$ and study the r -dependence of the corresponding ratio for sufficiently large τ . At small temperatures, this ratio will have an r -dependence that closely follows the r -dependence of the BS amplitude at $T = 0$. In Fig. 9, we compare $\phi_{\alpha}(\tau, T) = \tilde{C}_{\alpha}^r(\tau, T)/N_{\alpha}(\tau, T)$ for the lowest temperature, $T = 151$ MeV, and $\tau = 0.653$ fm with the corresponding zero temperature BS amplitudes. For the $\Upsilon(1S)$ and the $\Upsilon(2S)$, we do not see any difference between the zero tempera-

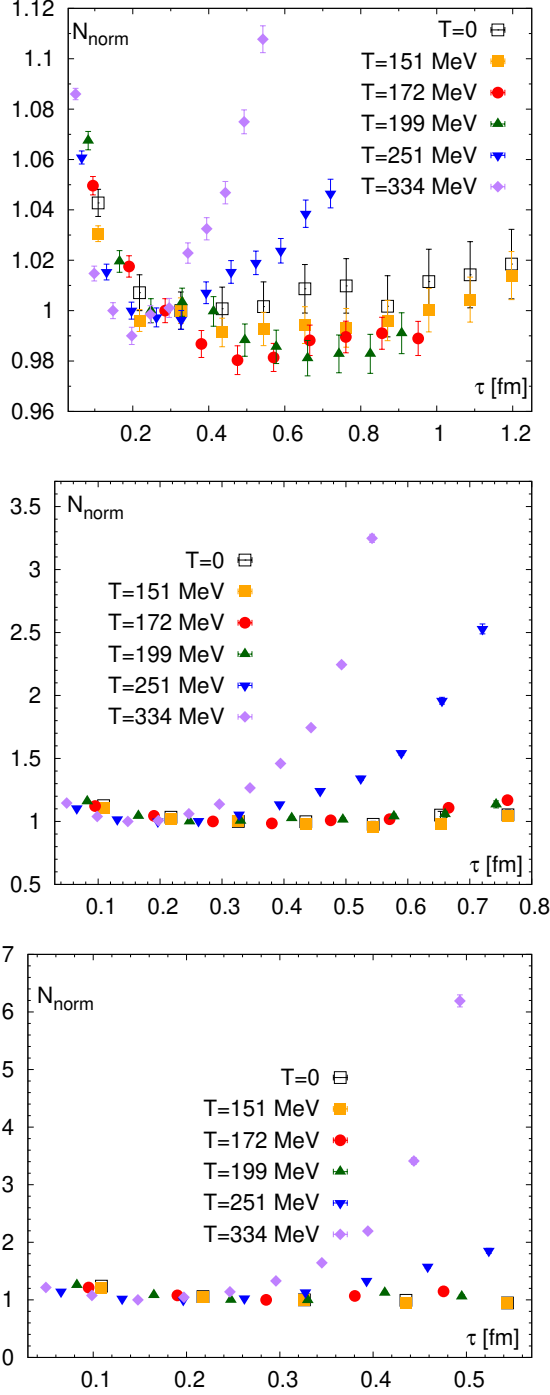


FIG. 7. Norm of the squared BS wave function at different temperatures for the $\Upsilon(1S)$ (Top), $\Upsilon(2S)$ (Middle) and $\Upsilon(3S)$ (Bottom) states.

ture BS amplitude and $\phi_\alpha(\tau, T)$. For the $\Upsilon(3S)$, some difference between the zero temperature and finite temperature result for $\phi_\alpha(\tau, T)$ can be seen at large r , though it is not statistically significant. In any case, the r -dependences of ϕ_α at $T = 0$ and $T = 151$ MeV are quite similar even for the $\Upsilon(3S)$. The lack of medium effects

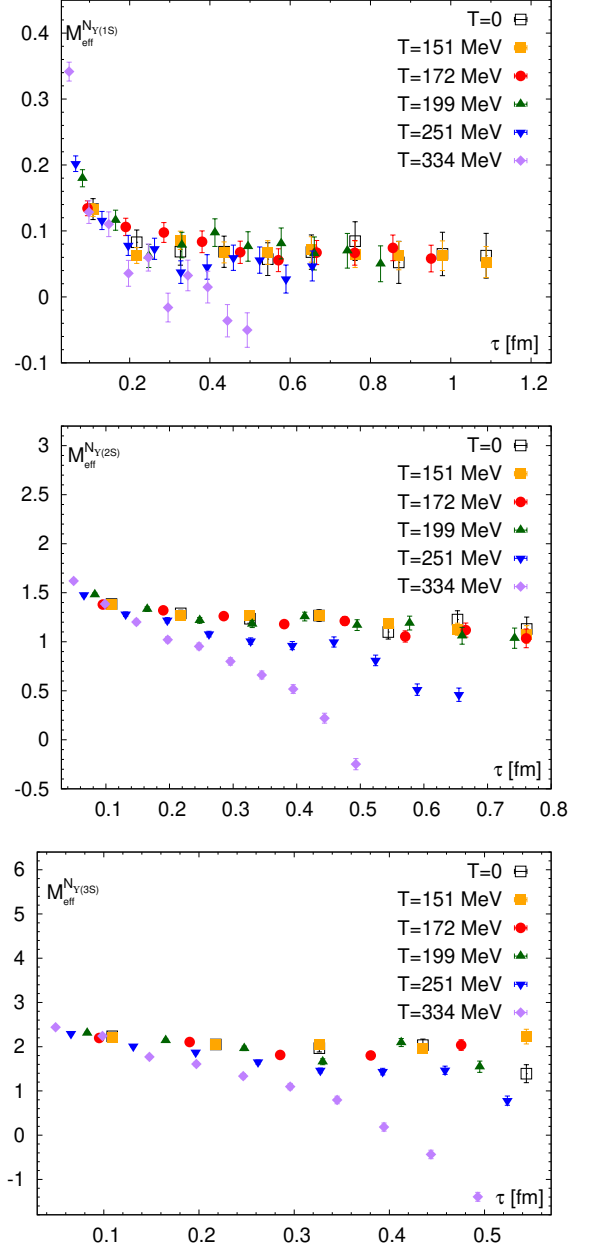


FIG. 8. Effective mass $M_{\text{eff}}^{N_\alpha}$ in GeV at different temperatures for $\Upsilon(1S)$ (Top), $\Upsilon(2S)$ (Middle) and $\Upsilon(3S)$ (Bottom) correlators.

in the BS amplitude for $T = 151$ MeV is not surprising since at this temperature all bottomonia should exist as well-defined states. Next, we compare $\phi_\alpha(\tau, T)$ at the lowest and the highest temperatures for τ around 0.4 fm. Namely, we use $\tau = 0.436$ fm at the lowest temperature and $\tau = 0.394$ fm at the highest temperature. This comparison is shown in Fig. 10, and no temperature effect can be observed. This is presumably due to the fact that for this τ value the contribution of the second term in Eq. (17) is too small. Therefore, in Fig. 11, we show our results for $\phi_\alpha(\tau, T)$ at $T = 251$ MeV and several values

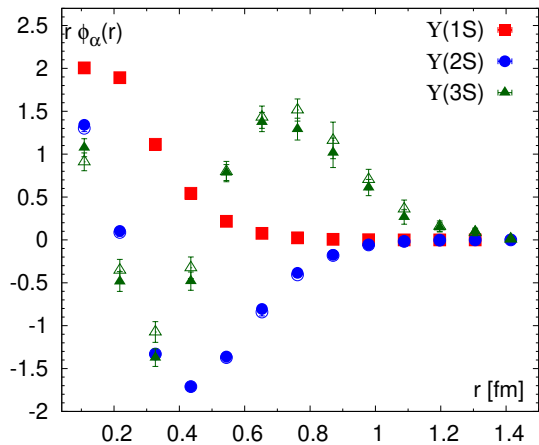


FIG. 9. The BS amplitudes times r for the $\Upsilon(1S)$, $\Upsilon(2S)$ and $\Upsilon(3S)$ at $T = 0$ MeV (filled symbols) and $T = 151$ MeV (open symbols) for $\tau = 0.653$ fm.

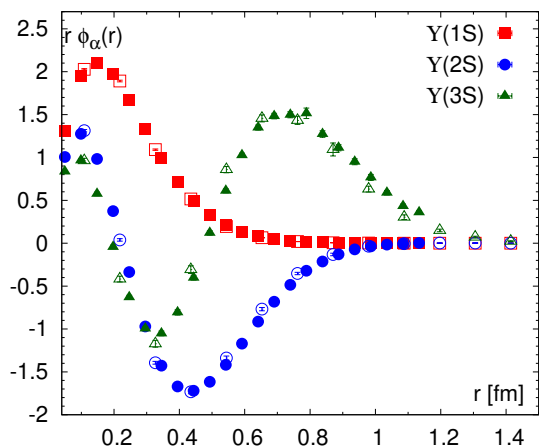


FIG. 10. BS amplitude times r for the $\Upsilon(1S)$, $\Upsilon(2S)$ and $\Upsilon(3S)$ at $T = 334$ MeV (filled symbols) and $T = 151$ MeV (open symbols) at $\tau \sim 0.4$ fm (see text).

of τ . As one can see from the figure for the $\Upsilon(2S)$ and $\Upsilon(3S)$, there is a significant τ -dependence of ϕ_α . At small r , the τ -dependence is mostly due to the τ -dependence of the normalization factor N_{norm} of the BS amplitude, cf. Fig. 7, while for larger r , also the shape of the BS amplitudes changes. This suggests that the normalized BS amplitude cannot be interpreted simply as the wave function of in-medium Υ in the potential model picture. Yet, the r dependence of $\phi_\alpha(\tau, T)$ does not change much from one τ value to another. In summary, the correlation $\tilde{C}_\alpha^r(\tau, T)$ shows significant temperature dependence as one would expect based on the previous studies. However, the r dependence of this correlator does not change significantly as the temperature and τ is varied. Thus, focusing only on the r dependence of $\tilde{C}_\alpha^r(\tau, T)$ without a detailed study of its τ dependence may result in wrong conclusions about the fate of $\Upsilon(2S)$ and $\Upsilon(3S)$ states at

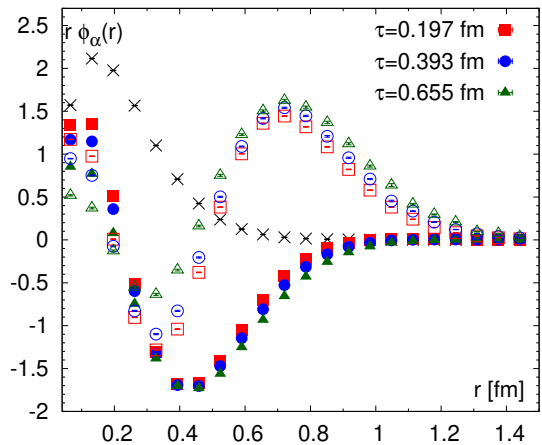


FIG. 11. The BS amplitude times r for the $\Upsilon(2S)$ (filled symbols) and $\Upsilon(3S)$ (open symbols) at $T = 251$ MeV for $\tau = 0.197$, 0.393 and 0.653 fm. Also shown as crosses is the result for the $\Upsilon(1S)$.

high temperature. For the $\Upsilon(1S)$, there is only little dependence of ϕ_α on τ , and therefore in Fig. 11, we only show the numerical results for $\tau = 0.393$ fm. This lack of τ -dependence indicates that $\Upsilon(1S)$ can exist in the deconfined medium at $T = 251$ MeV as a well defined state with little medium modification, in agreement with the previous studies of bottomonium at non-zero temperature based on NRQCD [44–49].

The lack of temperature dependence of the normalized BS amplitude at $T > 0$ at $\tau \simeq 0.4$ fm demonstrated in Fig. 10 has an interesting consequence. It means that $\phi_\alpha(r, T)$ can be used as a proxy for the $T = 0$ BS amplitude at zero temperature. Since the two temperatures shown in Fig. 10 correspond to two different lattice spacings this result also implies that the lattice spacing dependence of the BS amplitude is small. Therefore, the comparison of the wave function obtained from potential model and BS amplitude obtained on the lattice with $a = 0.1088$ fm in Section II seems justified.

V. CONCLUSIONS

Using lattice NRQCD in this paper, we studied the correlation functions, \tilde{C}_α^r , between operators optimized to have good overlaps with the of $\Upsilon(1S)$, $\Upsilon(2S)$, and $\Upsilon(3S)$ vacuum wave functions and simple spatially non-local bottomonium operators, where the bottom quark and anti-quark are separated by distance r . This correlator has been calculated at zero as well as at non-zero temperature. At zero temperature, \tilde{C}_α^r can be interpreted in terms of the Bethe-Salpeter amplitude. We have found that the r -dependence of the Bethe-Salpeter amplitude closely resembles the corresponding potential model based bottomonium wave function. Moreover, by choosing the bottom quark mass used in the Schrödinger

equation to be approximately 5.5 GeV we estimated the heavy quark antiquark potential from Bethe-Salpeter amplitudes and found agreement with the static quark potential calculated on the lattice. These findings support the potential model for the bottomonium in vacuum.

We studied the temperature and Euclidean time dependence of \tilde{C}_α^r in terms of effective masses. For $\Upsilon(1S)$, we see only very small temperature and Euclidean time dependence of the corresponding effective masses, except at the highest temperature of 334 MeV. For $\Upsilon(2S)$ and especially for $\Upsilon(3S)$ significant dependence on the Euclidean time were observed, making it difficult to draw parallels between Bethe-Salpeter amplitudes and potential model based in-medium wave functions. Since the r -dependence changes very little with varying Euclidean time and temperature, focusing solely on the r -dependence of \tilde{C}_α^r at a fixed τ might lead to misleading conclusions regarding existence of well-defined $\Upsilon(2S)$ and $\Upsilon(3S)$ in medium. On the other hand, we found that the behavior of the effective masses is similar to the one previously studied by us using correlators of optimized bottomonium operators [40], supporting the picture of

thermal broadening of bottomonium states.

ACKNOWLEDGMENTS

This material is based upon work supported by: (i) The U.S. Department of Energy, Office of Science, Office of Nuclear Physics and High Energy Physics through the Contract No. DE-SC0012704; (ii) The U.S. Department of Energy, Office of Science, Office of Nuclear Physics and Office of Advanced Scientific Computing Research within the framework of Scientific Discovery through Advance Computing (SciDAC) award Computing the Properties of Matter with Leadership Computing Resources. (iii) S. Meinel acknowledges support by the U.S. Department of Energy, Office of Science, Office of High Energy Physics under Award Number DE-SC0009913. (iv) Computations for this work were carried out in part on facilities of the USQCD Collaboration, which are funded by the Office of Science of the U.S. Department of Energy. (v) This research used awards of computer time provided by the INCITE and ALCC programs at Oak Ridge Leadership Computing Facility, a DOE Office of Science User Facility operated under Contract No. DE-AC05-00OR22725.

-
- [1] N. Brambilla *et al.* (Quarkonium Working Group), (2004), [arXiv:hep-ph/0412158 \[hep-ph\]](#).
 - [2] N. Brambilla *et al.*, *Eur. Phys. J.* **C71**, 1534 (2011), [arXiv:1010.5827 \[hep-ph\]](#).
 - [3] N. Brambilla, A. Pineda, J. Soto, and A. Vairo, *Nucl. Phys.* **B566**, 275 (2000), [arXiv:hep-ph/9907240 \[hep-ph\]](#).
 - [4] N. Brambilla, A. Pineda, J. Soto, and A. Vairo, *Rev. Mod. Phys.* **77**, 1423 (2005), [arXiv:hep-ph/0410047 \[hep-ph\]](#).
 - [5] W. Caswell and G. Lepage, *Phys. Lett. B* **167**, 437 (1986).
 - [6] Y. Ikeda and H. Iida, *Prog. Theor. Phys.* **128**, 941 (2012), [arXiv:1102.2097 \[hep-lat\]](#).
 - [7] T. Kawanai and S. Sasaki, *Phys. Rev. Lett.* **107**, 091601 (2011), [arXiv:1102.3246 \[hep-lat\]](#).
 - [8] T. Kawanai and S. Sasaki, *Phys. Rev.* **D85**, 091503 (2012), [arXiv:1110.0888 \[hep-lat\]](#).
 - [9] T. Kawanai and S. Sasaki, *Phys. Rev.* **D89**, 054507 (2014), [arXiv:1311.1253 \[hep-lat\]](#).
 - [10] K. Nochi, T. Kawanai, and S. Sasaki, *Phys. Rev.* **D94**, 114514 (2016), [arXiv:1608.02340 \[hep-lat\]](#).
 - [11] G. P. Lepage, L. Magnea, C. Nakhleh, U. Magnea, and K. Hornbostel, *Phys. Rev.* **D46**, 4052 (1992), [arXiv:hep-lat/9205007 \[hep-lat\]](#).
 - [12] B. A. Thacker and G. P. Lepage, *Phys. Rev.* **D43**, 196 (1991).
 - [13] C. T. H. Davies, K. Hornbostel, A. Langnau, G. P. Lepage, A. Lidsey, J. Shigemitsu, and J. H. Sloan, *Phys. Rev.* **D50**, 6963 (1994), [arXiv:hep-lat/9406017 \[hep-lat\]](#).
 - [14] S. Meinel, *Phys. Rev.* **D79**, 094501 (2009), [arXiv:0903.3224 \[hep-lat\]](#).
 - [15] S. Meinel, *Phys. Rev.* **D82**, 114502 (2010), [arXiv:1007.3966 \[hep-lat\]](#).
 - [16] T. C. Hammant, A. G. Hart, G. M. von Hippel, R. R. Horgan, and C. J. Monahan, *Phys. Rev. Lett.* **107**, 112002 (2011), [Erratum: *Phys. Rev. Lett.* **115**, 039901(2015)], [arXiv:1105.5309 \[hep-lat\]](#).
 - [17] R. J. Dowdall *et al.* (HPQCD), *Phys. Rev.* **D85**, 054509 (2012), [arXiv:1110.6887 \[hep-lat\]](#).
 - [18] J. O. Daldrop, C. T. H. Davies, and R. J. Dowdall (HPQCD), *Phys. Rev. Lett.* **108**, 102003 (2012), [arXiv:1112.2590 \[hep-lat\]](#).
 - [19] R. Lewis and R. M. Woloshyn, *Phys. Rev.* **D85**, 114509 (2012), [arXiv:1204.4675 \[hep-lat\]](#).
 - [20] M. Wurtz, R. Lewis, and R. M. Woloshyn, *Phys. Rev.* **D92**, 054504 (2015), [arXiv:1505.04410 \[hep-lat\]](#).
 - [21] T. Matsui and H. Satz, *Phys. Lett.* **B178**, 416 (1986).
 - [22] G. Aarts *et al.*, *Lorentz workshop: Tomography of the Quark-Gluon Plasma with Heavy Quarks Leiden, Netherlands, October 10-14, 2016*, *Eur. Phys. J.* **A53**, 93 (2017), [arXiv:1612.08032 \[nucl-th\]](#).
 - [23] A. Mocsy, P. Petreczky, and M. Strickland, *Int. J. Mod. Phys.* **A28**, 1340012 (2013), [arXiv:1302.2180 \[hep-ph\]](#).
 - [24] A. Bazavov, P. Petreczky, and A. Velytsky, “Quarkonium at Finite Temperature,” in *Quark-gluon plasma 4*, edited by R. C. Hwa and X.-N. Wang (2010) pp. 61–110, [arXiv:0904.1748 \[hep-ph\]](#).
 - [25] I. Wetzorke, F. Karsch, E. Laermann, P. Petreczky, and S. Stickan, *Nucl. Phys. Proc. Suppl.* **106**, 510 (2002), [arXiv:hep-lat/0110132 \[hep-lat\]](#).
 - [26] S. Datta, F. Karsch, P. Petreczky, and I. Wetzorke, *Phys. Rev.* **D69**, 094507 (2004), [arXiv:hep-lat/0312037 \[hep-lat\]](#).
 - [27] A. Jakovac, P. Petreczky, K. Petrov, and A. Velytsky, *Phys. Rev.* **D75**, 014506 (2007), [arXiv:hep-lat/0611017 \[hep-lat\]](#).

- [28] A. Mocsy and P. Petreczky, *Phys. Rev.* **D77**, 014501 (2008), [arXiv:0705.2559 \[hep-ph\]](#).
- [29] T. Umeda, R. Katayama, O. Miyamura, and H. Matsufuru, *Int. J. Mod. Phys.* **A16**, 2215 (2001), [arXiv:hep-lat/0011085 \[hep-lat\]](#).
- [30] H. Ohno, T. Umeda, and K. Kanaya (WHOT-QCD), *Proceedings, 26th International Symposium on Lattice field theory (Lattice 2008): Williamsburg, USA, July 14-19, 2008*, *PoS LATTICE2008*, 203 (2008), [arXiv:0810.3066 \[hep-lat\]](#).
- [31] T. Umeda, S. Ejiri, S. Aoki, T. Hatsuda, K. Kanaya, Y. Maezawa, and H. Ohno, *Proceedings, 26th International Symposium on Lattice field theory (Lattice 2008): Williamsburg, USA, July 14-19, 2008*, *PoS LATTICE2008*, 174 (2008), [arXiv:0810.1570 \[hep-lat\]](#).
- [32] H. Ohno, S. Aoki, S. Ejiri, K. Kanaya, Y. Maezawa, H. Saito, and T. Umeda (WHOT-QCD), *Phys. Rev.* **D84**, 094504 (2011), [arXiv:1104.3384 \[hep-lat\]](#).
- [33] P. W. M. Evans, C. R. Allton, and J. I. Skullerud, *Phys. Rev.* **D89**, 071502 (2014), [arXiv:1303.5331 \[hep-lat\]](#).
- [34] C. Allton, W. Evans, P. Giudice, and J.-I. Skullerud, (2015), [arXiv:1505.06616 \[hep-lat\]](#).
- [35] M. Laine, O. Philipsen, P. Romatschke, and M. Tassler, *JHEP* **03**, 054 (2007), [arXiv:hep-ph/0611300 \[hep-ph\]](#).
- [36] N. Brambilla, J. Ghiglieri, A. Vairo, and P. Petreczky, *Phys. Rev.* **D78**, 014017 (2008), [arXiv:0804.0993 \[hep-ph\]](#).
- [37] A. Bazavov *et al.*, *Phys. Rev.* **D85**, 054503 (2012), [arXiv:1111.1710 \[hep-lat\]](#).
- [38] A. Bazavov *et al.* (HotQCD), *Phys. Rev.* **D90**, 094503 (2014), [arXiv:1407.6387 \[hep-lat\]](#).
- [39] R. Larsen, S. Meinel, S. Mukherjee, and P. Petreczky, *Phys. Rev.* **D100**, 074506 (2019), [arXiv:1908.08437 \[hep-lat\]](#).
- [40] R. Larsen, S. Meinel, S. Mukherjee, and P. Petreczky, *Phys. Lett.* **B800**, 135119 (2020), [arXiv:1910.07374 \[hep-lat\]](#).
- [41] E. Eichten, K. Gottfried, T. Kinoshita, K. D. Lane, and T.-M. Yan, *Phys. Rev.* **D21**, 203 (1980).
- [42] S. Jacobs, M. G. Olsson, and C. Suchyta, III, *Phys. Rev.* **D33**, 3338 (1986), [Erratum: *Phys. Rev.* **D34**, 3536 (1986)].
- [43] G. S. Bali, K. Schilling, and A. Wachter, *Phys. Rev. D* **56**, 2566 (1997), [arXiv:hep-lat/9703019](#).
- [44] G. Aarts, S. Kim, M. P. Lombardo, M. B. Oktay, S. M. Ryan, D. K. Sinclair, and J. I. Skullerud, *Phys. Rev. Lett.* **106**, 061602 (2011), [arXiv:1010.3725 \[hep-lat\]](#).
- [45] G. Aarts, C. Allton, S. Kim, M. P. Lombardo, M. B. Oktay, S. M. Ryan, D. K. Sinclair, and J. I. Skullerud, *JHEP* **11**, 103 (2011), [arXiv:1109.4496 \[hep-lat\]](#).
- [46] G. Aarts, C. Allton, S. Kim, M. P. Lombardo, M. B. Oktay, S. M. Ryan, D. K. Sinclair, and J.-I. Skullerud, *JHEP* **03**, 084 (2013), [arXiv:1210.2903 \[hep-lat\]](#).
- [47] G. Aarts, C. Allton, T. Harris, S. Kim, M. P. Lombardo, S. M. Ryan, and J.-I. Skullerud, *JHEP* **07**, 097 (2014), [arXiv:1402.6210 \[hep-lat\]](#).
- [48] S. Kim, P. Petreczky, and A. Rothkopf, *Phys. Rev.* **D91**, 054511 (2015), [arXiv:1409.3630 \[hep-lat\]](#).
- [49] S. Kim, P. Petreczky, and A. Rothkopf, *JHEP* **11**, 088 (2018), [arXiv:1808.08781 \[hep-lat\]](#).